

# Studies of Photoinduced Electron Transfer and Energy Migration in a Conjugated Polymer System for Fluorescence “Turn-On” Chemosensor Applications

Li-Juan Fan and Wayne E. Jones, Jr.\*

Department of Chemistry, State University of New York at Binghamton, Binghamton, New York 13902

Received: November 4, 2005; In Final Form: February 8, 2006

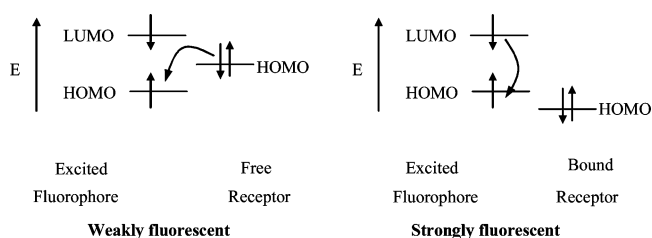
A series of poly[*p*-(phenyleneethynylene)-*alt*-(thienyleneethynylene)] (PPETE) polymers with variable percent loadings of the *N,N,N'*-trimethylethylenediamino group on the polymer backbone were synthesized and fully characterized. Photophysical studies show that changes in the loading of the amino group receptor on the backbone do not affect the polymer electronic structure in either the ground or excited states. The fluorescence quantum yields were found to be directly related to the loading of the amino groups and can be modeled by a Stern–Volmer type relationship. Photophysical studies related the total quenching efficiency to the inherent rate of photoinduced electron transfer (PET), the lifetime of the exciton, the rate of excitation energy migration along the polymer backbone, and the total loading of the receptor on the polymer. The role of the loading dependence on the application of these polymers as fluorescence “turn-on” sensors for toxic metal cations in dilute solution was also studied. Results showed that the fluorescence enhancement upon binding various cations was maintained even when the amino receptor loading along the polymer backbone was reduced.

## Introduction

Conjugated polymers have generated renewed enthusiasm in recent years because of their potential applications in organic light emitting diodes,<sup>1</sup> photovoltaics,<sup>2</sup> and many other fields. The wide range of applications is a result of the semiconducting and the fluorescence behaviors inherent to many of these systems. An exciting recent extension of these materials has been their subsequent application to fluorescent sensors.<sup>3</sup> Most of these applications have involved energy transfer along the polymer backbone resulting in enhanced fluorescence quenching in the presence of an analyte. A continuing challenge is the development of “turn-on” sensors in which fluorescence intensity increases in the presence of an analyte.

Numerous studies have been made on the properties and applications of conjugated polymers such as poly(*p*-phenylenevinylene) (PPV),<sup>4</sup> poly(*p*-phenyleneethynylene) (PPE),<sup>2,3,5</sup> polythiophene (PT)<sup>3a,c,6</sup> etc. Several groups have investigated the structure–property relationships of poly[*p*-(phenyleneethynylene)-*alt*-(thienyleneethynylene)]s (PPETEs) and their use as sensors.<sup>7,8</sup> The PPETEs have been found to be highly luminescent and also have very good processability. They deviate slightly from the PPE rigid-rod structure due to the inclusion of the five-member thiophene ring, but still have a relatively high degree of  $\pi$  electron delocalization.<sup>7</sup>

Our group has been exploring the use of poly[*p*-(phenyleneethynylene)-*alt*-(thienyleneethynylene)] (PPETE) as a conjugated polymer backbone for sensor application. Our previous work focused on functionalized PPETE as a fluorescence quenching chemosensor with different receptors capable of binding cations.<sup>8</sup> Recently, we extended our work to use PPETE in a conjugated polymer backbone as a fluorescence “turn-on” chemosensor, based on a photoinduced electron transfer (PET) quenching mechanism,<sup>9</sup> also referred to as charge shifting (Figure 1).

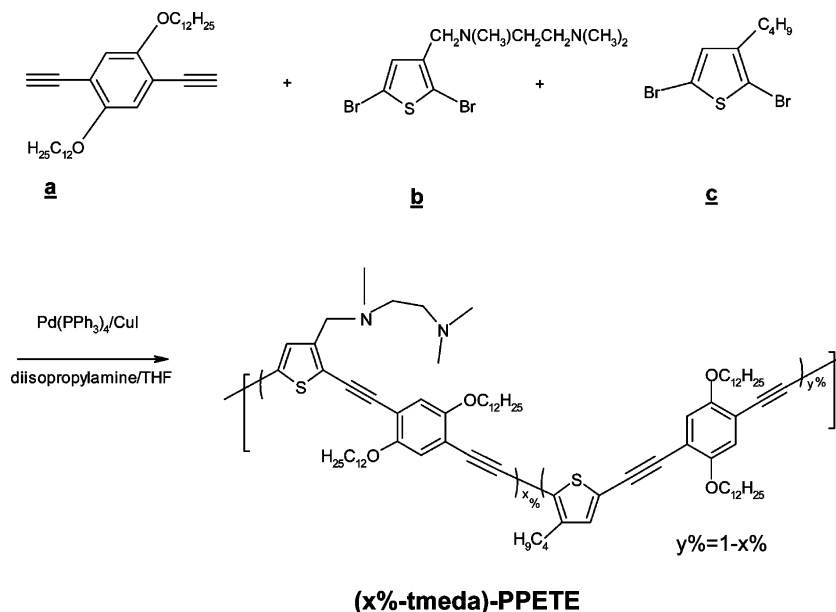


**Figure 1.** Orbital energy diagram for fluorescent PET sensors before and after cation binding.

In most PET systems, the fluorescence is quenched due to electron transfer between the excited fluorophore and a redox active receptor ligand. If the electron pair on the receptor atom is coordinated to some electron-deficient species such as a transition metal cation, the energy of the electron pair is lowered and the fluorescence will be turned on by the termination of the PET process. In our previous work,<sup>9</sup> we synthesized a tmeda-PPETE polymer with a poly[*p*-(phenyleneethynylene)-*alt*-(thienyleneethynylene)] backbone functionalized with the *N,N,N'*-trimethylethylenediamino group as the receptor. The receptor was in this case linked to the thiophene ring by a methylene spacer group. This system shows fluorescence enhancement upon binding protons,  $\text{Hg}^{2+}$ ,  $\text{Zn}^{2+}$ , and some other cations as their chloride salts. The employment of the PET strategy in conjugated polymers for “turn-on” sensor applications does not provide enhanced sensitivity as in conjugated polymer sensors involving a fluorescence quenching mechanism.<sup>3,8</sup> However, a fluorescence “turn-on” chemosensor against a “dark” background would reduce the likelihood of false positive signals upon binding analytes.<sup>10</sup> Further, conjugated polymers still have several advantages over small molecules as fluorescence “turn-on” sensors such as processability, feasibility to tune the electronic structure to meet system requirements, and enhanced selectivity of the system.<sup>8b</sup>

It can be argued that enhancement of sensitivity compared to small molecules is still possible with a PET “turn-on”

\* Address correspondence to this author. Phone: 607-777-2421. Fax: 607-777-4478. E-mail: wjones@binghamton.edu.

SCHEME 1: The Synthetic Route of (*x*%-tmeda)-PPETEs with Different Receptor Loading

conjugated polymer sensor. However, the factors which affect the sensitivity may be different from those in a “turn-off” system. Understanding the nature of these factors will be critical in the design of new conjugated polymer based “turn-on” sensors. One important issue is the efficiency of the PET process in this conjugated polymer backbone–receptor system. In a PET system, the HOMO-LUMO energy levels of the polymer fluorophore are very critical. The conjugated polymer backbone, unlike a simple small molecule, requires a common chain length for direct comparison because the HOMO-LUMO levels will change with the chain length. Another fundamental question about the PET based “turn-on” conjugated polymer system is how the intrachain energy transfer or energy migration along the polymer chain affects the total quenching of the polymer fluorescence by the receptor. To address these issues, a series of polymers were prepared with variable loading of the donor receptor unit as illustrated in Scheme 1, and subsequently denoted as (*x*%-tmeda)-PPETE. Here we report the synthesis and photophysical studies of this polymer series with the goal of investigating the PET process between the PPETE polymer backbone and the amino receptor as a function of loading. Further, the energy migration on the PPETE backbone and the effect of percent receptor loading on sensor sensitivity will be described.

### Experimental Section

**Materials.** 1,4-Diethynyl-2,5-didodecyloxybenzene<sup>11</sup> and *N*-(2,5-dibromothiophen-3-ylmethyl)-*N,N,N'*-trimethylethane-1,2-diamine<sup>9</sup> were synthesized according to the literature. 2,5-Dibromo-3-butylthiophene and all other materials were purchased from Aldrich and used as received unless otherwise noted.

**Measurements.** <sup>1</sup>H and <sup>13</sup>C NMR spectra were recorded on a Bruker AM-360 spectrometer. Elemental analyses were performed by QTI Inc. in New Jersey. IR spectra were obtained as KBr disks on a FTIR Bruker Equinox55 spectrophotometer at a nominal resolution of 2 cm<sup>-1</sup>. Molecular weights and distributions were determined by gel permeation chromatography (GPC), using a solution of 0.1% (by volume) triethylamine in toluene as the mobile phase at 40 °C and a flow rate of 0.5 mL/min, relative to polystyrene standards. The GPC instrument

was equipped with a Waters 510 pump, 410 differential refractive index detector, and Waters Styragel HT6, HT4, and HT2 (7.8 mm × 300 mm) columns. A pure toluene mobile phase was also carried out on the model PPETE for the comparison to previous studies. All samples analyzed by GPC gave monomodal distributions. UV–vis spectra were obtained on a Perkin-Elmer Lambda 2S spectrophotometer in tetrahydrofuran solution, using 1 cm quartz cuvette cells. Fluorescence spectra were measured on a SLM 48000s spectrofluorometer, using excitation at 410 nm with 4 nm slits. The fluorescence solutions were prepared as described previously.<sup>8b</sup> All the cationic solutions (Hg<sup>2+</sup>, Zn<sup>2+</sup>, H<sup>+</sup>) were prepared by dissolving their chlorides in water. Fluorescence quantum yields were determined in anhydrous argon degassed THF, relative to quinine sulfate in 0.5 M H<sub>2</sub>SO<sub>4</sub> solutions with a reference quantum yield of 0.546, excited at 365 nm.<sup>7b</sup> The experiments were repeated three times and the final value of the quantum yields was reported as the average within a deviation of ±0.01. Lifetime data were obtained by time-correlated single photon counting at the University of Pennsylvania. The experiment details were the same as described previously.<sup>8b</sup>

**Synthesis of (*x*%-tmeda)-PPETEs with Different Receptor Percent Loading.** All copolymers were synthesized according to the procedure described in detail for tmeda-PPETE.<sup>9</sup> The key difference was the feed ratio of monomer **b** (*N*-(2,5-dibromothiophen-3-ylmethyl)-*N,N,N'*-trimethylethane-1,2-diamine) and monomer **c** (2,5-dibromo-3-butylthiophene). The experimental description is illustrated here in detail for the (50%-tmeda)-PPETE as an example; complete synthetic details are available in the Supporting Information.

**(50%-tmeda)-PPETE.** Diisopropylamine (2 mL) was added to a mixture of 1,4-diethynyl-2,5-didodecyloxybenzene (0.494 g, 1.00 mmol), *N*-(2,5-dibromothiophen-3-ylmethyl)-*N,N,N'*-trimethylethane-1,2-diamine (0.178 g, 0.50 mmol), 2,5-dibromo-3-butylthiophene (0.149 g, 0.50 mmol), Pd(PPh<sub>3</sub>)<sub>4</sub> (58 mg, 0.050 mmol), and CuI (20 mg, 0.10 mmol) in 10 mL of anhydrous THF under an argon atmosphere. The mixture was refluxed for 24 h, and then 20 mL of chloroform was added. The organic phase was washed twice with dilute NaHCO<sub>3</sub> solution followed by two washes with H<sub>2</sub>O. The solvent was removed under reduced pressure and the residue was washed with hot water

**TABLE 1: Theoretical and Measured Percentages of Nitrogen in (x%-tmeda)-PPETE**

|                   | tmeda-PPETE | (50%-tmeda)-PPETE | (25%-tmeda)-PPETE | (12.5%-tmeda)-PPETE | model PPETE |
|-------------------|-------------|-------------------|-------------------|---------------------|-------------|
| theoretical (% N) | 4.05        | 2.09              | 1.07              | 0.54                | 0           |
| found (% N)       | 3.69        | 1.77              | 0.95              | 0.45                | 0           |

and hot methanol. The crude product was dissolved in chloroform and then precipitated in methanol twice and dried under vacuum to give an orange-yellow solid (0.502 g, yield 76%).  $^1\text{H}$  NMR (360 MHz,  $\text{CDCl}_3$ ):  $\delta_{\text{H}}$  6.9–7.2(3H), 4.0 (4H), 3.4–3.7 (1H), 2.5–2.8 (1H), 2.1–2.3 (4.5 H), 0.8–1.9 (49.5 H) ppm. FTIR ( $\text{cm}^{-1}$ ): 2922, 2853, 2816, 2764, 2192, 1494, 1455, 1214, 1030. GPC:  $M_w$   $1.60 \times 10^4$ ,  $M_n$   $1.03 \times 10^4$ . PDI: 1.68.

## Results and Discussion

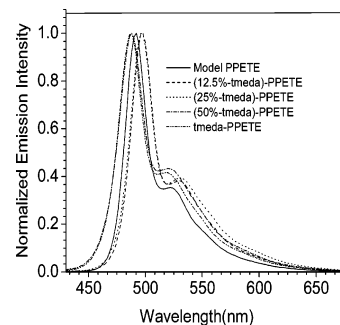
**Synthesis.** The synthesis of all polymers proceeded similar to that of the tmeda-PPETE system described in detail previously.<sup>9</sup> The strategy in this work was to use different monomer feed ratios to evaluate the role of receptor loading. The polymers were prepared by a step growth polymerization employing palladium-catalyzed cross-coupling<sup>12</sup> of 1,4-diethynyl-2,5-didodecyloxybenzene (monomer **a**), *N*-(2,5-dibromothiophen-3-ylmethyl)-*N,N,N'*-trimethylethane-1,2-diamine (monomer **b**), and 2,5-dibromo-3-butylthiophene (monomer **c**) as shown in Scheme 1. It is important to note that we assume the thiophene units with and without receptor to be randomly distributed due to the nature of the polymerization method employed.

Monomer **a** was synthesized from 1,4-hydroquinone in four steps as described in the literature.<sup>11</sup> Monomer **b** was synthesized in three steps from commercially available 3-methylthiophene.<sup>9</sup> Monomer **c** was commercially available from Aldrich and was used directly. All of the (x%-tmeda)-PPETE and model PPETE polymers were obtained in relatively high yields of around 80% in the polymerization step. The solubility in common solvents such as THF and toluene increased with decreasing receptor loading.

All polymers were well-characterized by NMR, FTIR, and GPC (see the Supporting Information). The elemental nitrogen analysis provided proof of the amino receptor loading in these polymers, consistent with the theoretical value (Table 1). These values were calculated according to the feed ratio and average molecular weight obtained from gel permeation chromatography (GPC).

**Polymer Photophysics.** The absorption and emission spectra of the (x%-tmeda)-PPETEs are very similar to those of the model PPETE within experimental error (Figures 2 and 3). Previous studies<sup>8</sup> showed that the absorption at 452 nm in these polymers can be assigned to the  $\pi-\pi^*$  transition in the polymer backbone and the emission maximum at 488 nm and the shoulder at 530 nm can be attributed to a single electronic transition with vibronic structure. The model polymer we used

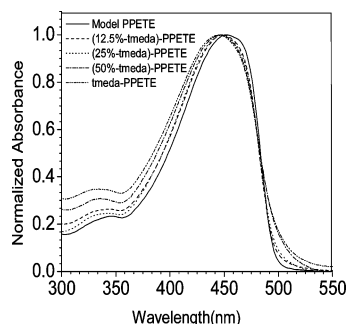
here was slightly different from previous reports,<sup>8,9</sup> since here we use a butyl group on the thiophene ring instead of a dodecyl side chain. This was done based on the consideration that the butyl group was much closer to the *N,N,N'*-trimethylethane-1,2-diamino group in length. Given the similarity in the photophysical properties we conclude that these variations do not significantly influence the electronic structure of the lowest energy electronic transitions.

**Figure 3.** Emission spectra of (x%-tmeda)-PPETEs in THF.

The photophysical data for (x%-tmeda)-PPETEs are shown in Table 2. The fluorescence quantum yield of the polymers decreased from 0.26 to 0.09 with increasing loading of the amino receptors compared to the model polymer. This was consistent with the expected electron-transfer quenching of the  $\pi-\pi^*$  excited state by the receptor.

It is interesting to note that even for the 100% receptor loaded polymer, tmeda-PPETE, the fluorescence was not completely quenched. Several reasons could be used to describe this residual fluorescence.<sup>13,14</sup> The first involves a kinetic competition between the regular fluorescence and the intramolecular PET process. When the PET quenching rate is slow, significant fluorescence can be observed. The second possibility involves the presence of localized fluorescence domains that are not coupled to a receptor. The receptor is expected to be randomly distributed along the polymer chain. The receptor loaded thiophene monomer and the 3-alkyl thiophene monomer are expected to have the same reactivity in the polymerization process based on the similarity in their structure. In this scenario, localized fluorescence domains should increase with decreasing percent loading of the amino group.

A plot of the quantum yields of fluorescence versus percent loading of the receptors on every *p*-(phenyleneethynylene)-*alt*-(thienyleneethynylene) (PETE) unit fits well with a first-order exponential decay as shown in Figure 4. This result is consistent with the localized fluorescence domains argument above. The exponential decrease of the fluorescence with increasing con-

**Figure 2.** Absorption spectra of (x%-tmeda)-PPETEs in THF.**TABLE 2: Photophysical Properties of (x%-tmeda)-PPETEs in THF Solution at Room Temperature**

|                     | UV-vis<br>( $\lambda_{\text{max}}$ , nm) |     | emission<br>( $\lambda_{\text{max}}$ , nm) |     | quantum<br>yield |
|---------------------|--|-----|--|-----|------------------|
| (100%-tmeda)-PPETE  | 334                                      | 446 | 488  | 520 | 0.09             |
| (50%-tmeda)-PPETE   | 336                                      | 448 | 488  | 520 | 0.13             |
| (25%-tmeda)-PPETE   | 344                                      | 448 | 496  | 530 | 0.17             |
| (12.5%-tmeda)-PPETE | 344                                      | 448 | 496  | 530 | 0.19             |
| model PPETE         | 346                                      | 452 | 492  | 522 | 0.26             |

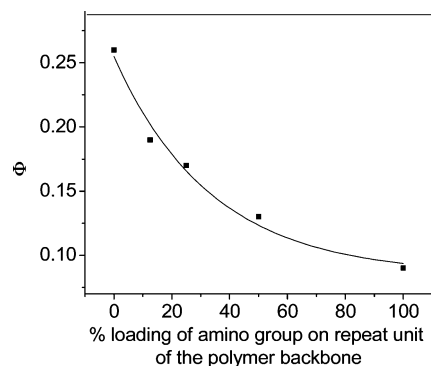


**Figure 4.** Quantum yields of fluorescence vs percent loading of amino groups in (*x*%-tmeda)-PPETEs.

centration of the amino group is also expected in this model. Miller et al systematically investigated a noncovalent linked donor–acceptor system in solid solution. In those systems, the distance between the donor and acceptor was fixed.<sup>15</sup> The acceptor fluorescence was found to decrease exponentially with increasing the donor concentration. This was attributed to the randomly distributed donor and acceptor in the solid and the residual fluorescence came from those fluorophores outside the quenching sphere of the quenchers. By analogy in our system, localized fluorescence domains would be outside the quenching sphere of the exciton.

Emission lifetimes were evaluated by single-photon counting following 408 nm excitation. The emission decay was best fit to a biexponential function for all polymers with 0.5 and 0.2 ns components. The decays could also be fit to exponential distribution functions with a similar number of fitting parameters as observed previously for multicomponent polymers systems.<sup>14</sup> The lifetimes showed no significant differences among these polymers including the relative ratio of the two biexponential components. The invariant lifetimes are also consistent with the residual fluorescence resulting from localized fluorescence domains discussed above.

#### Photoinduced Electron Transfer and Energy Migration

**Analysis.** The invariance of the emission lifetime provides insight into the quenching mechanism for the polymer chemosensors. For small molecules, there are two classifications of quenching mechanisms: dynamic quenching and static quenching.<sup>16</sup> If the quencher irreversibly binds to the fluorophore before excitation, a new absorption, relaxation, or energy transfer process is created that favors quenching. This is called static quenching. If the quencher molecule interacts with the fluorophore through collision, this is termed dynamic quenching. Given that the amino groups are covalently bound to the PPETE fluorophore before excitation, the static quenching mechanism was expected. The observed lack of change in the emission lifetime with change in the amino group loading in (*x*%-tmeda)-PPETEs is consistent with the static quenching mechanism.<sup>16a</sup> This also suggests that there is limited kinetic competition between the regular fluorescence and the intramolecular PET process.

While the static quenching mechanism is consistent with our data, there are two significant differences between our (*x*%-tmeda)-PPETE system and small molecule PET systems. The first difference is that the excitation energy can be described as a delocalized exciton that spreads over several repeat units along the polymer backbone. The degree of the delocalization of the excitation energy could be decided by the polymer composition, structural defects, or electronic factors. On the basis of the similarity of the absorption and emission spectra and

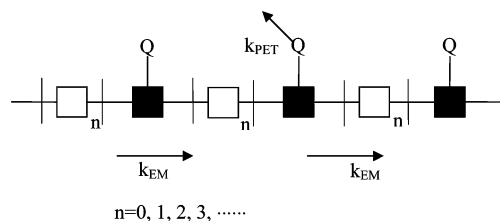


**Figure 5.** Representation of process leading to energy-migration enhanced quenching with a PET mechanism along the conjugated polymer backbone.

emission lifetime of this (*x*%-tmeda)-PPETE series, we conclude that all polymers have similar exciton length. Further, this would indicate that there is no significant difference in the photoinduced electron-transfer driving force for the quenching within the series since the quencher is the same in all cases.<sup>17,18</sup>

Another distinctive characteristic of conjugated polymer systems is that the exciton could travel along the polymer backbone through energy transfer, or more accurately, energy migration. This energy migration process can lead to additional quenching of the polymer beyond the static process. This has previously been assigned to the bimodal quenching in the fluorescent polymer chemosensor system.<sup>8b</sup> Some graphical models have been reported in the literature to describe the excitation energy migration and quenching mechanism. A modified model for our system is illustrated in Figure 5.<sup>8b,19</sup> The total quenching efficiency in this model is decided by the rate of energy migration ( $k_{EM}$ ) along the polymer chain and the PET quenching rate.

Webber et al.<sup>19</sup> have described the case of a quencher residing permanently on a fluorescent polymer. The relative rates between quenching and energy migration have an effect on the total efficiency of the quenching process. If the energy migration is much slower than the quenching rate,  $k_{EM} \ll k_{PET}$ , any exciton locally excited at the quencher site or reaching the quencher site by energy migration is immediately quenched. Hence the energy migration on the polymer backbone improves the total quenching efficiency.

If the energy migration is faster than the quenching rate,  $k_{EM} \geq k_{PET}$ , the energy migration may remove the exciton from the quencher site before quenching takes place. The energy migration enhanced quenching might not be observed. This situation is very similar to a dynamic quenching process induced by the diffusion in small bimolecular systems. The only difference is that in our case the exciton “diffuses” through energy migration instead of the quencher diffusing to the fluorophore. This situation cannot be true in the (*x*%-tmeda)-PPETE system because it is known that the dynamic quenching would lead to a decreased lifetime with increasing quencher loading. Since the lifetimes are invariant, we can conclude that  $k_{EM} \ll k_{PET}$  in this system.

To further understand the PET quenching of the polymer fluorescence by the amino group, an alternative analysis was undertaken with the Stern–Volmer quenching formalism in our system. Figure 6 shows the Stern–Volmer fluorescence quantum yield ratios for the model PPETE as a function of the percent loading of the amino group. All the data can be fit to a linear relationship, similar to Stern–Volmer quenching in a bimolecular fluorophore–quencher system.<sup>16</sup>

From the linear Stern–Volmer quenching in Figure 6 and the fact that the polymer fluorescence lifetime has no amino loading dependence, we can deduce that the energy migration cannot be very fast within the emissive lifetime. Otherwise, a small amount of the amino group would quench the polymer



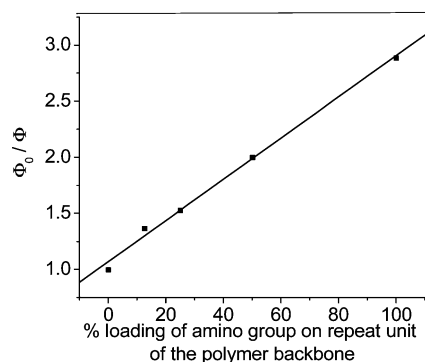


**Figure 6.** Quantum yield ratios between the model PPETE and (*x*%-tmeda)-PPETE vs percent loading of the amino group.

**TABLE 3: Maximum Fluorescence Enhancement for (*x*%-tmeda)-PPETEs upon Titration of Different Cations**

|                     | Hg <sup>2+</sup> | H <sup>+</sup> | Zn <sup>2+</sup> |
|---------------------|------------------|----------------|------------------|
| (100%-tmeda)-PPETE  | 2.65             | 1.87           | 1.68             |
| (50%-tmeda)-PPETE   | 2.36             | 2.29           | 2.00             |
| (25%-tmeda)-PPETE   | 2.02             | 2.02           | 1.60             |
| (12.5%-tmeda)-PPETE | 2.23             | 2.21           | 2.04             |

fluorescence completely. However, energy migration enhanced fluorescence quenching was still observed in (*x*%-tmeda)-PPETE, since the fluorescence of 12.5% amino receptor loaded polymer was quenched by 27%, according to the quantum yields. If we correct for the residual fluorescence, 12.5% amino receptor actually quenched about 41% quenchable fluorescence of the polymer backbone.<sup>20</sup> From this set of observations we conclude that  $k_{EM} \leq 1/\tau_0$  ( $\sim 10^9$  s<sup>-1</sup>)  $\ll k_{PET}$ .

**Cation Titrations.** A fundamental question is the relative sensitivity between the polymers and complementary small molecule sensors. From the photophysical data, it is clear that variations in the receptor on the PPETE conjugated polymer backbone result in variations in the fluorescence intensity. A reduction of receptor loading on a polymer chain increases the distance between the receptors and excitons on average. At the low loading limit the polymer will behave as a small molecule with a single fluorophore–receptor pair. Unlike the high sensitivity in fluorescence “turn-off” chemosensors, conjugated polymer fluorescence “turn-on” sensors are not expected to demonstrate the same level of fluorescence sensitivity enhancement. However, if the excitation energy migration rate is relatively large and the exciton lifetime is long, an increase in sensitivity for the conjugated polymer compared to small molecule sensors may still be observed.

To investigate the sensitivity of these new chemosensory polymers with variable receptor loading, the influence of various cations (Hg<sup>2+</sup>, Zn<sup>2+</sup>) and protons on the fluorescence behavior of (*x*%-tmeda)-PPETEs was investigated. All the polymers, except the model PPETE, had similar responses toward each cation and the results are summarized in Table 3. Figure 7 is a representative figure of the fluorescence enhancement of the polymer in THF solution upon addition of cations to the (50%-tmeda)-PPETE. These results were consistent with previous reports on this system.<sup>9</sup> The overall quenching efficiency at high concentrations was limited by the persistent background fluorescence mentioned above. However, at low concentrations the steep slope of the quenching curve resulted in detectable fluorescence changes at concentrations on the nM level (see the Supporting Information).

When titrated with Hg<sup>2+</sup>, the fluorescence of all the (*x*%-tmeda)-PPETEs increased sharply at low concentration (<5  $\mu$ M). The fluorescence enhancements changed more gradually

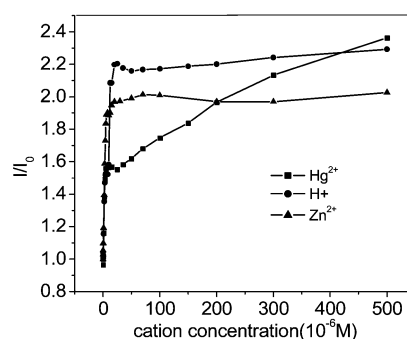


**Figure 7.** Fluorescence enhancement of (50%-tmeda)-PPETE in THF upon addition of cations. In these experiments the polymer concentration was held at a constant 5  $\mu$ M in repeat unit of the polymer backbone.

upon further addition of Hg<sup>2+</sup>. Even when the concentration of Hg<sup>2+</sup> reached the highest concentration studied (0.5 mM), the fluorescence enhancement continued. The response toward Zn<sup>2+</sup> with all the (*x*%-tmeda)-PPETEs was distinctly simple. The fluorescence enhancement reached saturation at very low cation concentration (about 5  $\mu$ M) and did not increase further with addition of larger concentrations.

The situation is more complicated in the case of protonation. In response to decreasing pH, the increase in fluorescence in all of the (*x*%-tmeda)-PPETEs had two stages (see the Supporting Information, Figure 5S). The fluorescence enhancement initially reached saturation at low concentration (<5  $\mu$ M). Upon continuing the titration, the fluorescence intensity became constant and then increased again at a higher concentration before leveling off at the largest concentrations studied (0.5 mM). This bimodal response is likely due to the fact that one amino receptor can accommodate two protons, since the *N,N,N'*-trimethylethylenediamino group has two nitrogens. Another possibility may include interchain interactions. However, there is negligible shift in energy or band shape for all the emission spectra of (*x*%-tmeda)-PPETEs. Further investigation is needed to clarify the exact protonation mechanism. Nonetheless, these results clearly support a cation-based selectivity for each of the ions tested.

From Table 3 the maximum fluorescence enhancements for (*x*%-tmeda)-PPETEs at different receptor loading show no large variation upon binding the same cation. In an ideal PET conjugated polymer–receptor system, in which PET quenching is very efficient and the energy migration is very rapid within the lifetime, the maximum enhancement of fluorescence should be the same for all the (*x*%-tmeda)-PPETEs. Thus, in this fluorescence “turn-on” system, diluting the receptor along the polymer chain did not change the intensity enhancement of fluorescence. In addition the concentration of each cation reaching maximum fluorescence enhancement or saturation is almost the same for different polymers (see the Supporting Information). Thus the sensitivity did not increase by reducing the receptor loading as expected in an ideal conjugated polymer with the PET system as a fluorescence “turn-on” system. This could be attributed to the limited energy migration along the polymer backbone as discussed previously. Higher sensitivity may be achieved in systems with better energy migration along the polymer backbone.

## Conclusion

We have successfully synthesized a series of (*x*%-tmeda)-PPETE (*x* = 0, 12.5, 25, 50, 100) polymers as fluorescence “turn-on” chemosensors for dissolved cations. Photophysical studies of these polymers show that the relative loading of the

amino group has negligible structural or electronic distortion of the polymer backbone in the ground or excited state. Analysis of the fluorescence quantum yields vs the percent loading of the amino group on the polymer followed Stern–Volmer behavior usually found between fluorophores and quenchers in bimolecular small molecule systems. Considering the same PET driving force for all the ( $x\%$ -tmeda)-PPETEs, the amino group loading dependence of the fluorescence suggested that the energy migration along the polymer backbone must be relatively slow. Cation titrations of this series of polymers showed no sensitivity enhancements with reduced receptor loading. The sensitivity toward cations was consistent with the relatively sluggish energy migration along the polymer backbone.

**Acknowledgment.** The authors thank Dr. Brendan R. Flynn and Dr. Stanley K. Madan for the careful review of this manuscript. The authors would also like to thank Dr. Thomas Troxler for the lifetime experiments at the University of Pennsylvania. This research was funded by a grant from the National Institutes of Health (NIH grant 1R15ES10106-01).

**Supporting Information Available:** Synthesis, characterizations (NMR and FTIR spectra, GPC data) of all polymers and corresponding discussion, cartoon explanations of an ideal PET system for sensor application, and  $I/I_0$  vs cation concentration curves for all ( $x\%$ -tmeda)-PPETEs and enlarged parts of  $I/I_0$  vs cation concentration curve at low cation concentration. This material is available free of charge via the Internet at <http://pubs.acs.org>.

## References and Notes

- (1) (a) Burroughes, J. H.; Bradley, D. D. C.; Brown, R. N.; Marks, R. N.; Friend, R. H.; Burns, P. L.; Holmes, A. B. *Nature* **1990**, *347*, 539. (b) Burn, P. L.; Kraft, A.; Baigent, D. R.; Bradley, D. D. C.; Brown, A. R.; Friend, R. H.; Gymer, R. W.; Holmes, A. B.; Jackson, R. W. *J. Am. Chem. Soc.* **1993**, *115*, 10117. (c) Kraft, A.; Grimsdale, A. C.; Holmes, A. B. *Angew. Chem., Int. Ed.* **1998**, *37*, 402. (d) Friend, R. H.; Gymer, R. W.; Holmes, A. B.; Burroughes, J. H.; Marks, R. N.; Taliani, C.; Bradley, D. D. C.; Dos Santos, D. A.; Brédas, J. L.; Lögdlund, M.; Salaneck, W. R. *Nature* **1999**, *397*, 121. (e) Heeger, A. J. *Angew. Chem., Int. Ed.* **2001**, *40*, 2591. (f) Zhao H. C.; Sanda, F.; Masuda, T. *Macromolecules* **2004**, *37*, 8893. (g) Fan, Q. L.; Lu, S.; Lai, Y. H.; Hou, X. Y.; Huang, W. *Macromolecules* **2003**, *36*, 6976. (h) Ding, L.; Lu, Z.; Egbe, D. A. M.; Karasz, F. E. *Macromolecules* **2004**, *37*, 10031.
- (2) (a) Arango, A. C.; Carter, S. A.; Brock, P. J. *Appl. Phys. Lett.* **1999**, *74*, 1698. (b) Arango, A. C.; Johnson, L. R.; Bliznyuk, V. N.; Schlesinger, Z.; Carter, S. A.; Horhold, H. H. *Adv. Mater.* **2000**, *12*, 1689. (c) McDonald, S. A.; Konstantatos, G.; Zhang, S. G.; Cyr, P. W.; Klem, E. J. D.; Levina, L.; Sargent, E. H. *Nat. Mater.* **2005**, *4*, 138. (d) Coakley, K. M.; McGehee, M. D. *Chem. Mater.* **2004**, *16*, 4533. (e) Ramos, A. M.; Rispens, M. T.; van Duren, J. K. J.; Hummelen, J. C.; Janssen, R. A. J. *J. Am. Chem. Soc.* **2001**, *123*, 6714.
- (3) (a) Swager, T. M. *Acc. Chem. Res.* **1998**, *31*, 201. (b) Zhou, Q.; Swager, T. M. *J. Am. Chem. Soc.* **1995**, *117*, 12593. (c) McQuade, D. T.; Pullen, A. E.; Swager, T. M. *Chem. Rev.* **2000**, *100*, 2537. (d) Gaylord, B. S.; Massie, M. R.; Feinstein, S. C.; Bazan, G. C. *Proc. Natl. Acad. Sci. U.S.A.* **2005**, *102*, 34. (e) Kumaraswamy, S.; Bergstedt, T.; Shi, X. B.; Rininsland, F.; Kushon, S.; Xia, W. S.; Ley, K.; Achuthan, K.; McBranch, D.; Whitten, D. *Proc. Natl. Acad. Sci. U.S.A.* **2004**, *101*, 7511. (f) Wang, S.; Gaylord, B. S.; Bazan, G. C. *J. Am. Chem. Soc.* **2004**, *126*, 5446.
- (4) (a) Petrella, A.; Tamborra, M.; Curri, M. L.; Cosma, P.; Striccoli, M.; Cozzoli, P. D.; Agostiano, A. *J. Phys. Chem. B* **2005**, *109*, 1554. (b) Dwight, S. J.; Gaylord, B. S.; Hong, J. W.; Bazan, G. C. *J. Am. Chem. Soc.* **2004**, *126*, 16850. (c) Watt, A.; Thomsen, E.; Meredith, P.; Rubinsztein-Dunlop, H. *Chem. Commun.* **2004**, *21*, 2490. (d) Yu, Z. H.; Barbara, P. F. *J. Phys. Chem. B* **2004**, *108*, 11321. (e) Karabunarliev, S.; Bittner, E. R. *J. Phys. Chem. B* **2004**, *108*, 10219.
- (5) (a) Khan, A.; Muller, S.; Hecht, S. *Chem. Commun.* **2005**, *5*, 584. (b) Nakashima, H.; Furukawa, K.; Ajito, K.; Kashimura, Y.; Torimitsu, K. *Langmuir* **2005**, *21*, 511. (c) DiCesare, N.; Pinto, M. R.; Schanze, K. S.; Lakowicz, J. R. *Langmuir* **2002**, *18*, 7785. (d) Kushon, S. A.; Ley, K. D.; Bradford, K.; Jones, R. M.; McBranch, D.; Whitten, D. *Langmuir* **2002**, *18*, 7245.
- (6) (a) Duvail, J. L.; Retho, P.; Fernandez, V.; Louarn, G.; Molinie, P.; Chauvet, O. *J. Phys. Chem. B* **2004**, *108*, 18552. (b) Ho, H. A.; Leclerc, M. *J. Am. Chem. Soc.* **2004**, *126*, 1384. (c) Jousset, B.; Lanchard, P.; Levillain, E.; de Bettignies, R.; Roncali, J. *Macromolecules* **2003**, *36*, 3020. (d) Ho, H. A.; Boissinot, M.; Bergeron, M. G.; Corbeil, G.; Dore, K.; Boudreau, D.; Leclerc, M. *Angew. Chem., Int. Ed.* **2002**, *41*, 1548. (e) Levesque, I.; Bazinet, P.; Roovers, J. *Macromolecules* **2000**, *33*, 2952.
- (7) (a) Li, J.; Pang, Y. *Macromolecules* **1998**, *31*, 5740. (b) Pang, Y.; Li, J.; Barton, T. J. *J. Mater. Chem.* **1998**, *8*, 1686.
- (8) (a) Zhang, Y.; Murphy, C. B.; Jones, W. E., Jr. *Macromolecules* **2002**, *35*, 630. (b) Murphy, C. B.; Zhang, Y.; Troxler, T.; Ferry, V.; Martin, J. J.; Jones, W. E., Jr. *J. Phys. Chem. B* **2004**, *108*(5), 1537.
- (9) Fan, L. J.; Zhang, Y.; Jones, W. E., Jr. *Macromolecules* **2005**, *38*, 2844.
- (10) (a) McQuade, D. T.; Hegedus, A. H.; Swager, T. M. *J. Am. Chem. Soc.* **2000**, *122*, 12389. (b) Rurack, K.; Kollmannsberger, M.; Resch-Genger, U.; Daub, J. *J. Am. Chem. Soc.* **2000**, *122*, 968.
- (11) Swager, T. M.; Gil, C. J.; Wrighton, M. S. *J. Phys. Chem.* **1995**, *99*, 4886.
- (12) Yamamoto, T.; Honda, K.; Ooba, N.; Tomaru, S. *Macromolecules* **1998**, *31*, 7.
- (13) Ghosh, P.; Bharadwaj, P. K.; Jayanta, R.; Ghosh, S. *J. Am. Chem. Soc.* **1997**, *119*, 11903.
- (14) Guillet, J. *Polymer Photophysics and Photochemistry*; Cambridge University Press: Cambridge, UK, 1985.
- (15) Miller, J. R.; Peeples, J. R.; Schmitt, M. J.; Closs, G. L. *J. Am. Chem. Soc.* **1982**, *104*, 6488.
- (16) (a) Lakowicz, J. R. *Principle of Fluorescence Spectroscopy*, 2nd ed.; Kluwer Academic/Plenum Publishers: New York, 1999; p 238. (b) Turro, N. J. *Modern Molecular Photochemistry*; University Science Books: Sausalito, CA, 1991; p 247.
- (17) (a) de Silva, A. P.; Gunaratne, H. Q. N.; Lynch, P. L. M.; Patten, A. J.; Spence, G. L. *J. Chem. Soc., Perkin Trans. 2* **1993**, 1611. (b) Jones, G., II; Griffin, S. F.; Choi, C. Y.; Bergmark, W. R. *J. Org. Chem.* **1984**, *49*, 2705. (c) de Silva, A. P.; Gunaratne, H. Q. N.; Gunnlaugsson, T.; Huxley, A. J.; McCoy, C. P.; Rademacher, J. T.; Rice, T. E. *Chem. Rev.* **1997**, *97*, 1515. (d) Valeur, B.; Leray, I. *Coord. Chem. Rev.* **2000**, *205*, 3. (e) Huston, M. E.; Haider, K. W.; Czarnik, A. W. *J. Am. Chem. Soc.* **1988**, *110*, 4460.
- (18) (a) Rehm, D.; Weller, A. *Isr. J. Chem.* **1970**, *8*, 259. (b) Weller, A. *Pure Appl. Chem.* **1968**, *16*, 115.
- (19) Itoh, Y.; Kamioka, K.; Webber, S. E. *Macromolecules* **1989**, *22*, 2851.
- (20) Apparent fluorescence quenching for (12.5%-tmeda) =  $(\phi_0 - \phi_{12.5})/\phi_0 \approx 0.27 = 27\%$ . Considering the residual fluorescence when the 100% amino group was loaded, the percent fluorescence quenching =  $(\phi_0 - \phi_{12.5})/(\phi_0 - \phi_{100}) \approx 0.41 = 41\%$ .  $\phi_x$  denotes the quantum yield of fluorescence of ( $x\%$ -tmeda)-PPETE.